Special issue of the 2nd International Conference on Computational and Experimental Science and Engineering (ICCESEN 2015)

Experimental Characterization of Antimony Dopant in Silicon Substrate

H. Serrar[a], R. Labbani[a,*] and C. Benazzouz[b]

[a]Laboratoire de Physique Mathématique et Subatomique, Département de Physique, Faculté des Sciences Exactes, Université Mentouri de Constantine, Route de Ain El Bey, 25000 Constantine, Algeria

[b]Centre de Développement des Techniques Nucléaires, 2 Bd Frantz Fanon, BP 399, Alger Gare, Algeria

Ion implantation is a method largely used to fabricate shallow junctions in the surface target. However, the ions are randomly redistributed and a huge damage is generated in the sample. Annealing treatments are thus necessary to restore defects and to activate the dopant. Among several elements, antimony is particularly attractive since it has low diffusivity in silicon which means that is suitable to obtain ultra shallow junctions. Moreover, antimony is attractive in many applications such as the fabrication of transistors and infrared detectors. In this work, the electrical activation of antimony is studied in case of silicon target.

DOI: 10.12693/APhysPolA.130.51

PACS/topics: 61.72.U–, 68.55.Ln, 85.40.Ry

1. Introduction

Ion implantation is a doping method widely employed in semiconductor technology for the fabrication of several bipolar devices in silicon substrates particularly. This technique enables to inject a controllable quantity of any element into the near-surface region of any substrate with a good accuracy [1]. Antimony is a dopant suitable for the fabrication of n-type ultrashallow junctions (i.e. thickness < 0.1 μm). This is due to its high mass and low diffusivity in silicon [2–4]. However, it is reported that antimony atoms are generally out-diffused from silicon substrates at high temperature annealing [5, 6]. The phenomenon of out-diffusion which is obviously accompanied by a loss in dopant dose, has been noticed for both $\langle 100 \rangle$ and $\langle 111 \rangle$ oriented silicon substrates. In another study, it was found that the maximum electrical activity and considerable decrease in the concentration of defects were achieved at a temperature around 620 °C [7].

In this work, the Rutherford backscattering spectroscopy (RBS) technique was mainly carried out to study the behaviour of antimony atoms implanted in silicon targets. Moreover, the method has been employed to investigate the re-growth of silicon damaged layers which were generated by antimony implantation. By using RBS in channelling mode, we were able to compute the quantity of antimony atoms which were redistributed, in substitutional silicon lattice, by annealing treatment. This quantity is called F_s and it is computed via the formula (1) [8, 9]:

$$F_s = \frac{1 - \chi_{\min}^{\mathrm{Sb}}}{1 - \chi_{\min}^{\mathrm{Si}}}, \tag{1}$$

where $\chi_{\min}^{\mathrm{Sb}}$ — minimum yield for impurity (Sb), $\chi_{\min}^{\mathrm{Si}}$ — minimum yield for crystal (Si).

*corresponding author; e-mail: labbanire@gmail.com

To study and simulate RBS data, we have used the RBX code [10] which is a program allowing us to compute ion implantation parameters (projected range R_p, standard deviation ΔR_p, etc.). The code was particularly interesting since it was able to simulate RBS spectra in channelling mode and to obtain the profile of defects which were generated by ion implantation in the target. For comparison reason, the stopping and range of ions in matter (SRIM) software [11, 12] has also been used to estimate the ion implantation parameters. Finally, electrical measurements have been carried out to study the electrical behaviour of antimony atoms in the silicon substrates.

2. Experimental

In this work, Si (111) substrates were implanted with Sb^+ ions, at room temperature, with energy of 120 keV at different doses (Table I). Afterwards, annealing treatment was performed at 900 °C during 30 min under vacuum ($P = 10^{-6}$ Torr).

TABLE I

Illustration of experimental conditions performed for each sample.

Samples	Dose [10^{15} Sb^+/cm^2]	Thermal annealing
virgin	0	/
S1	1	annealed
S2	1	non-annealed
S3	1.6	non-annealed
S4	1.6	annealed

The analysing of samples was performed by RBS technique, using a Van de Graaf accelerator producing He^+ particles with energy of 2 MeV. The technique was carried out in random and channelling modes. For channelling measurements, He^+ beam was parallel to the crystallographic axis of Si(111) sample. Concerning the angular scan, it was performed in an interval of ±1°.

The electrical analysis was based on resistivity measurements. It was carried out in an apparatus of "EPS-08 Alessi" type. This device was equipped with four points (of tungsten alloy) which were aligned and equidistant ($S = 1$ mm). The current used between the outer probes was 0.3 mA.

3. Results and discussion

In Fig. 1, we display RBS spectra (antimony signals only) in random mode for S1–S4 samples. It is clear that the signals (corresponding to non-annealed samples) possess areas significantly greater than that related to annealed specimens. This means that a huge loss of antimony has occurred by exo-diffusion, from silicon substrates, after annealing treatment. This phenomenon is in agreement with our previous work which was performed in other conditions but with the same species (i.e. antimony) [6, 13]. Using RBX code, the simulation of antimony signal of sample S2 has shown that the maximum of antimony concentration was situated at 613 Å below the surface compared with the projected range (R_p) of 641 Å (found by SRIM program).

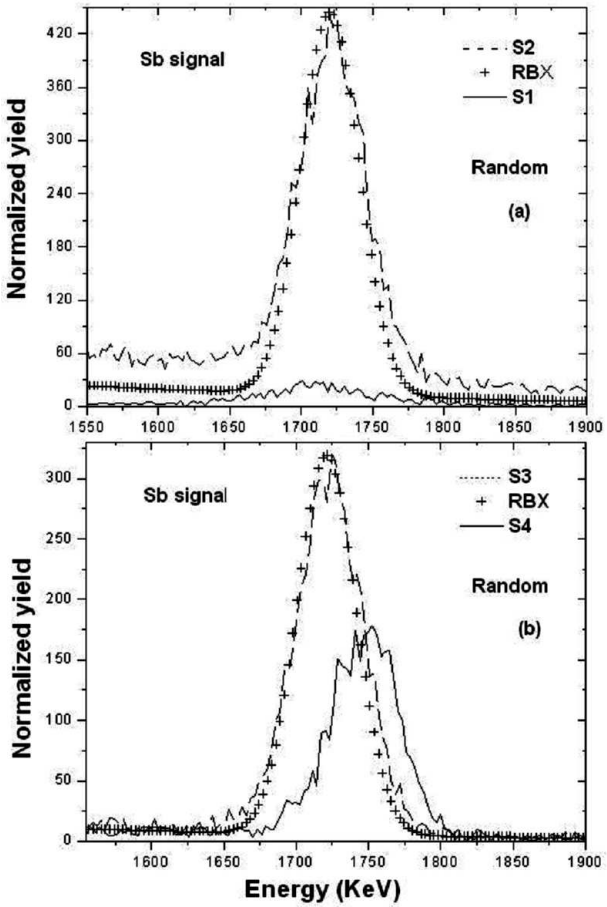

Fig. 1. RBS spectra for annealed (S1, S4) and non-annealed (S2, S3) samples in random mode. Only antimony signals are displayed.

We also found a dose of 0.85×10^{15} Sb^+ cm^{-2} compared with the nominal dose of 1×10^{15} Sb^+ cm^{-2} and a concentration of 7.59×10^{19} Sb^+ cm^{-3} which is superior with respect to maximum solid solubility of Sb in silicon (i.e. 7×10^{19} Sb^+ cm^{-3}) reported in literature [14, 15]. For Fig. 1b similar results have been obtained. The experimental dose of Sb atoms was approximately equal to 1.18×10^{15} Sb^+ cm^{-2} and the concentration was $\approx 1.24 \times 10^{20}$ Sb^+ cm^{-3} which was higher than the reported maximum solid solubility of Sb in Si. For the projected range, we obtained a value of 583 Å that was in good agreement with that provided by SRIM code.

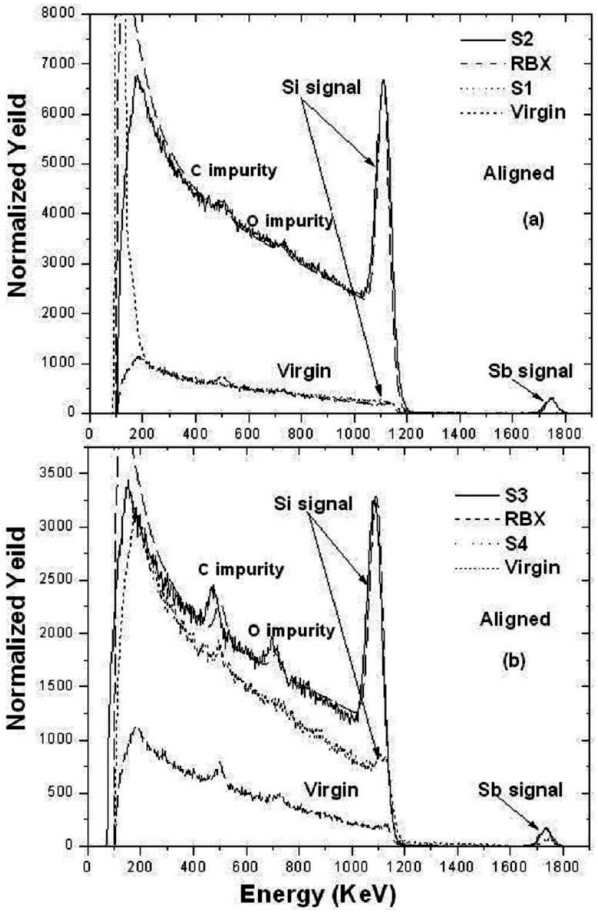

Fig. 2. RBS spectra for annealed (S1, S4) and non-annealed (S2, S3) samples in channeling mode.

In Fig. 2a and b the analysis by RBS in channelling mode of as-implanted samples (S2, S3) exhibited very high surface peaks (with respect to virgin sample ($\cdots$)). This is related to significant radiation damage generated by ion implantation in the targets. After the annealing treatment, a good recovery of radiation damage has been obtained. This is revealed by the channelling spectrum of Fig. 2a ($\cdots$) which became comparable to that related to virgin sample (i.e. reference spectrum). Concerning the case of Fig. 2b, corresponding to the higher

dose, the restoration of radiation damage was not completed. Indeed, the surface peak of annealed sample really decreased but was not superposed with the channelling spectrum of virgin specimen. The simulation of aligned spectra (by RBX code) has been performed for all samples. For illustration, in Fig. 2a and b the simulated spectra are displayed for non-annealed samples. According to these simulated spectra (which are well superposed with the experimental) one can conclude the accuracy of the program.

The restoration of radiation damage is better revealed by the defects profiles which were deduced by RBX code from Fig. 2. Indeed, in Fig. 3, the obtained profiles for non-annealed samples (S2, S3) exhibited significantly higher concentrations than those related to annealed specimens (S1, S4).

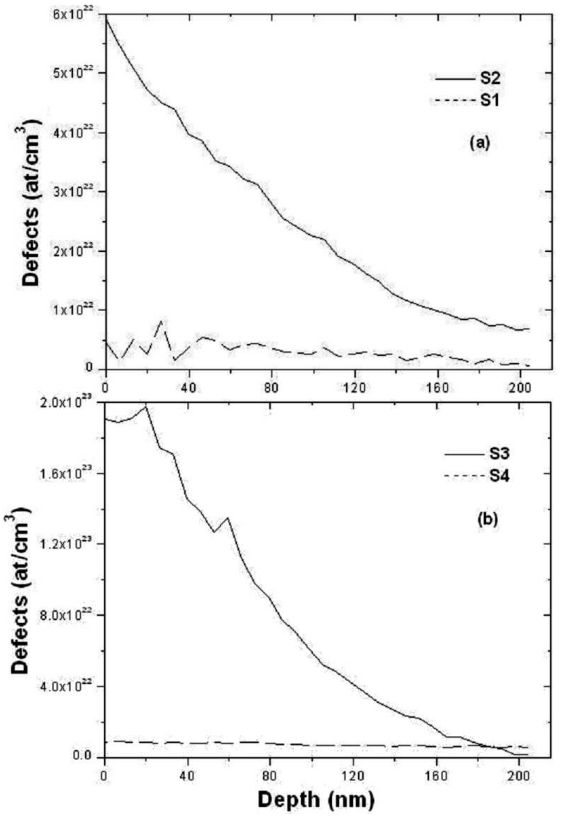

Fig. 3. Defects profiles deduced by RBX code from channeling RBS spectra of Fig. 2.

To study the redistribution of antimony atoms in Si(111) substrates, we have used the channeling wells obtained by RBS, in channeling mode, following $\langle 111 \rangle$ main axis (Fig. 4). For as-implanted samples (S2, S3), the angular distribution was almost linear which means that antimony atoms were randomly localized in the target. After the annealing treatment, the wells formation became deeper and more narrowed which is attributed to the migration of antimony atoms to substitutional positions in silicon target.

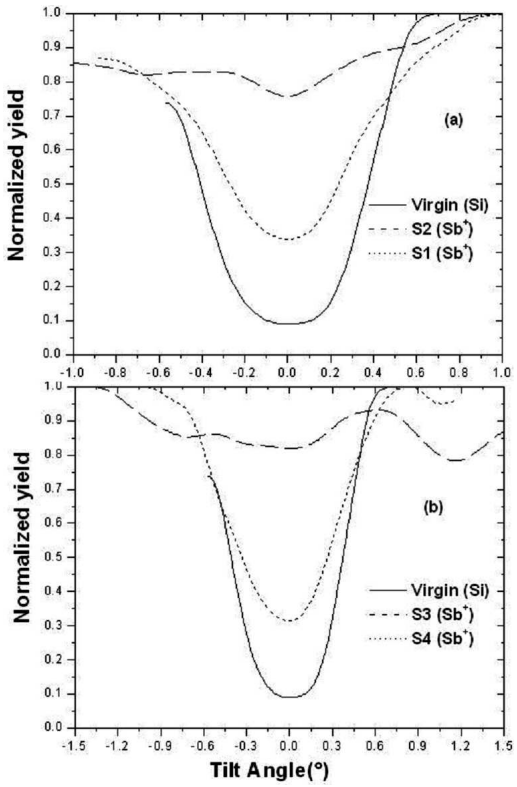

Fig. 4. Channeling angular distribution for Si and Sb around $\langle 111 \rangle$ axis for annealed (S1, S4) and non-annealed (S2, S3) samples.

To study the electrical activation of antimony atoms in the targets, we plot in Fig. 5 the resistivity of samples with respect to the quantity F_s computed via formula (1). The resistivity was found to be inversely proportional to F_s which is logical since the resistivity is known to be inversely proportional to the number of active careers. According to Fig. 5, one can also conclude that the majority of Sb atoms have been redistributed to substitutional positions in Si targets where they became electrically active. This result is in agreement with literature [16].

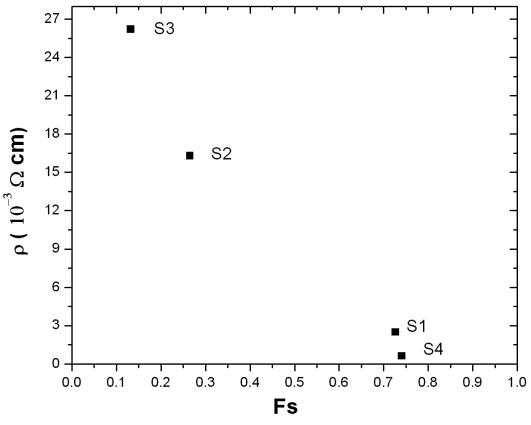

Fig. 5. Resistivity of the different samples with respect to F_s parameter.

In Fig. 6, we display the variations of resistivity as a function of each specimen. The resistivity obtained from the virgin is approximately equal to 6.456×10^{-3} Ω cm. This low value indicates that the material was not very resistive which was due to the intrinsic properties of the used semiconductor material. After ion implantation of Sb^+ ions in Si(111) targets (Fig. 6a), the resistivity jumped until 16.284×10^{-3} Ω cm and 26.21×10^{-3} Ω cm for S2 and S3 samples respectively. This was probably due to the amorphisation of samples, by Sb^+ ions implantation, which was more significant for the high dose. After the annealing treatment (Fig. 6b), the resistivity decreased significantly and achieved $\approx 2.497 \times 10^{-3}$ Ω cm and $\approx 0.637 \times 10^{-3}$ Ω cm for S1 and S4 samples respectively. The decrease is logically attributed to the electrical activation of antimony dopant by heat treatment [17] which is a satisfactory result.

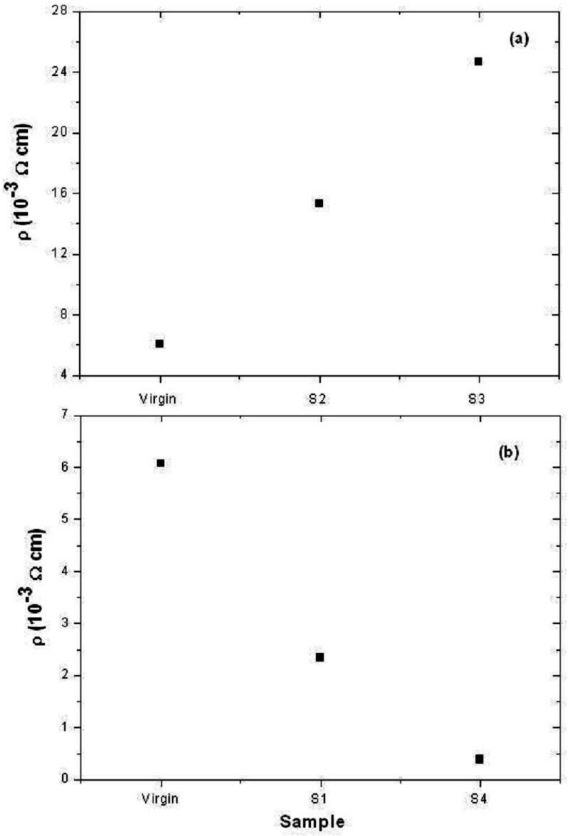

Fig. 6. Variations of resistivity with respect to different samples.

4. Conclusion

In the present paper, we have studied the behavior of antimony atoms implanted in silicon targets. The combination of electrical measurements and the Rutherford backscattering analysis has allowed important information concerning the position and the electrical activation of the dopant. The main results of our study were in agreement with literature and can be summarized as follows.

- In non annealed samples, no electrical activation has been noticed.
- The antimony migration to substitutional silicon lattice was observed for annealed specimens only.
- The fraction of substituted antimony atoms (F_s) was computed with a good accuracy.
- The fraction F_s increased while the resistivity of samples decreased.

Acknowledgments

The authors would like to thank Professor Endre Kotai, from Nuclear Physics Laboratory in KFKI institute (Budapest), for providing the RBX code.

References

[1] H. Herman, J.K. Hirvonen, *Treatise on Materials Science and Technology, Ion Implantation*, Academic Press, New York 1980.

[2] G.A. Sai-Halasz, H.B. Harrison, *IEEE Electr. Dev. Lett.* **7**, 534 (1986).

[3] E. Murakami, K. Harada, D. Hisamoto, S. Kimura, in: *Electron Devices Meeting, IEDM '96, International*, IEEE, San Francisco 1996, p. 439.

[4] K. Shibahara, K. Egusa, K. Kamesaki, H. Furomoto, *Jpn. J. Appl. Phys.* **39**, 2194 (2000).

[5] C. Revenant-Brizard, J.R. Regnard, S. Solmi, A. Armigliato, S. Valmorri, C. Cellini, F. Romanato, *J. Appl. Phys.* **79**, 12 (1996).

[6] R. Labbani, R. Halimi, *Mater. Sci. Eng. B* **124–125**, 208 (2005).

[7] C. Benazzouz, N. Boussaa, S. Behli, M. Zilabdi, S. Tobbech, M. Derdour, *Alg. Rev. Nucl. Sci.* **2**, 119 (1997).

[8] J.A. Borders, J.M. Poate, *Phys. Rev. B* **13**, 969 (1976).

[9] W.K. Chu, J.W. Mayer, M.A. Nicolet, *Backscattering Spectroscopy*, Academic Press, New York 1978.

[10] E. Kotai, *Nucl. Instrum. Methods Phys. Res. B* **85**, 588 (1994).

[11] J.P. Biersack, L.G. Haggmark, *Nucl. Instrum. Methods* **174**, 257 (1980).

[12] J.F. Ziegler, *The Stopping and Range of Ions in Matter/TRansport of Ions in Matter, SRIM/TRIM Code*, www.srim.org.

[13] R. Labbani, R. Halimi, T. Laoui, A. Vantomme, B. Pipeleers, G. Roebben, *Mater. Sci. Eng. B* **102**, 390 (2003).

[14] J. Narayan, O.W. Holland, *Physica Status Solidi A* **73**, 225 (1982).

[15] A. Sato, K. Suzuki, H. Horie, T. Sugii, in: *Proc. IEEE Int. Conf. Microelectron. Test Struct.*, IEEE, Nara 1995, p. 259.

[16] J.F. Letcher, J. Narayan, O.W. Holland, *Inst. Phys. Conf. Ser.* **60**, 265 (1981).

[17] J.S. Williams, *Nucl. Instrum. Methods* **209/210**, 219 (1983).